Journal of Molecular Liquids 384 (2023) 122260

Contents lists available at ScienceDirect

Journal of Molecular Liquids

journal homepage: www.elsevier.com/locate/molliq

A first-principal study of pure and encapsulation boron nitride cluster with alkaline metals as the metformin drug carrier

Ying Lai [a,*], Tariq J. Al-Musawi [b], Uday Abdul-Reda Hussein [c], Ibrahem Waleed [d], Hanan Hassan Ahmed [e], Anwar Qasim Khallawi [f], Khulood Majid Alsaraf [g], Mohammed Asiri [h], Munther Abosaooda [i], Hashem O. Alsaab [j]

[a] Department of Life Science and Agriculture, Zhoukou Normal University, Zhoukou, Henan 466001, China
[b] Building and Construction Techniques Engineering Department, Al-Mustaqbal University College, 51001 Hillah, Babylon, Iraq
[c] College of Pharmacy, University of Al-Ameed, Iraq
[d] Medical Technical College, Al-Farahidi University, Iraq
[e] Department of Pharmacy, Al-Noor University College, Nineveh, Iraq
[f] Medical Technical College, National University of Science and Technology, Dhi Qar, Iraq
[g] Medical Technical College, Al-Esraa University College, Baghdad, Iraq
[h] Department of Clinical Laboratory Sciences, College of Applied Medical Sciences, King Khalid University, Abha, Saudi Arabia
[i] College of Pharmacy, the Islamic University, 54001 Najaf, Iraq
[j] Department of Pharmaceutics and Pharmaceutical Technology, Taif University, Taif 21944, Saudi Arabia

ARTICLE INFO

Keywords:
Drug delivery
Computational simulation
Nanocarrier
Boron Nitride

ABSTRACT

Finding new drug-delivery materials has attracted considerable interest from many researchers in recent years. Herein, systematic investigation of the metformin interaction with the surface of pristine $B_{12}N_{12}$ and group I metals (Li, Na, and K) encapsulation nanoclusters was carried out at B3LYP/631++ (d, p) level of theory based on the DFT calculations. MF molecule has two nucleophilic sites, NH and NH_2 groups. The trapping of Li, Na, and K atoms affected the HOMO–LUMO gaps of the considered configurations and the electronic properties of considered complexes. Besides, it is noticed that presence of alkali metals remarkably increased the absorption energies of MF-$B_{12}N_{12}$ to −2.14, −2.24, −2.30, and −2.38 for $B_{12}N_{12}$, Li@$B_{12}N_{12}$, Na@$B_{12}N_{12}$, and K@$B_{12}N_{12}$ respectively. In addition, DOS plots show a decrease in E_{gap} by the addition of alkali metals and therefore an increase in reactivity of the considered configurations, which is confirmed by the decrease in total hardness.

1. Introduction

Metformin ($C_4H_{11}N_5$) (MF) drug is utilized to decrease blood sugar amount in patients with type 2 diabetes [1,2]. It works by decreasing the absorption of glucose from the intestines, lowering glucose production in the liver, and improving insulin sensitivity. In addition, researchers are investigating metformin's potential to reduce the risk of cancer [3–5], dementia, and stroke, slow aging, prevent age-related diseases, and increase lifespan in people with type 2 diabetes. On the other hand, by using MF, LDL cholesterol and triglycerides in the blood are reduced. Therefore, MF is an essential and useful drug for the medicine of diabetics, and it's easier absorption into the blood is very important.

In the last decades, many nanostructures have been introduced as drug delivery systems due to their unique features such as small particle size, higher drug loading capacity, and controllable release profile in the field [6,7]. Carbon fullerene nanostructures [8–11], boron nitride clusters, and nanotubes have drawn considerable attention because of their remarkable physical and chemical characteristics. Boron nitride nanomaterials are more stable than carbon nanomaterials from the chemical point of view and compared to carbon nanostructures, boron nitride nanomaterials have superior chemical inertness, making them viable candidates for biomedical applications [12,13]. Based on previous studies $B_{12}N_{12}$ is the most stable cluster between (BN)s structures [14]. Fowler et al. [15] calculations indicated that the $B_{12}N_{12}$, $B_{16}N_{16}$, and $B_{28}N_{28}$ are magic clusters of the boron nitride and the $B_{12}N_{12}$ cluster is the more stable. Also, computational studies showed that the $B_{12}N_{12}$ structure includes of eight hexagonal and six square rings, and is more durable than one that contains hexagons and pentagons [16,17]. In

* Corresponding author.
E-mail address: 20041026@zknu.edu.cn (Y. Lai).

https://doi.org/10.1016/j.molliq.2023.122260
Received 8 May 2023; Received in revised form 29 May 2023; Accepted 2 June 2023
Available online 4 June 2023

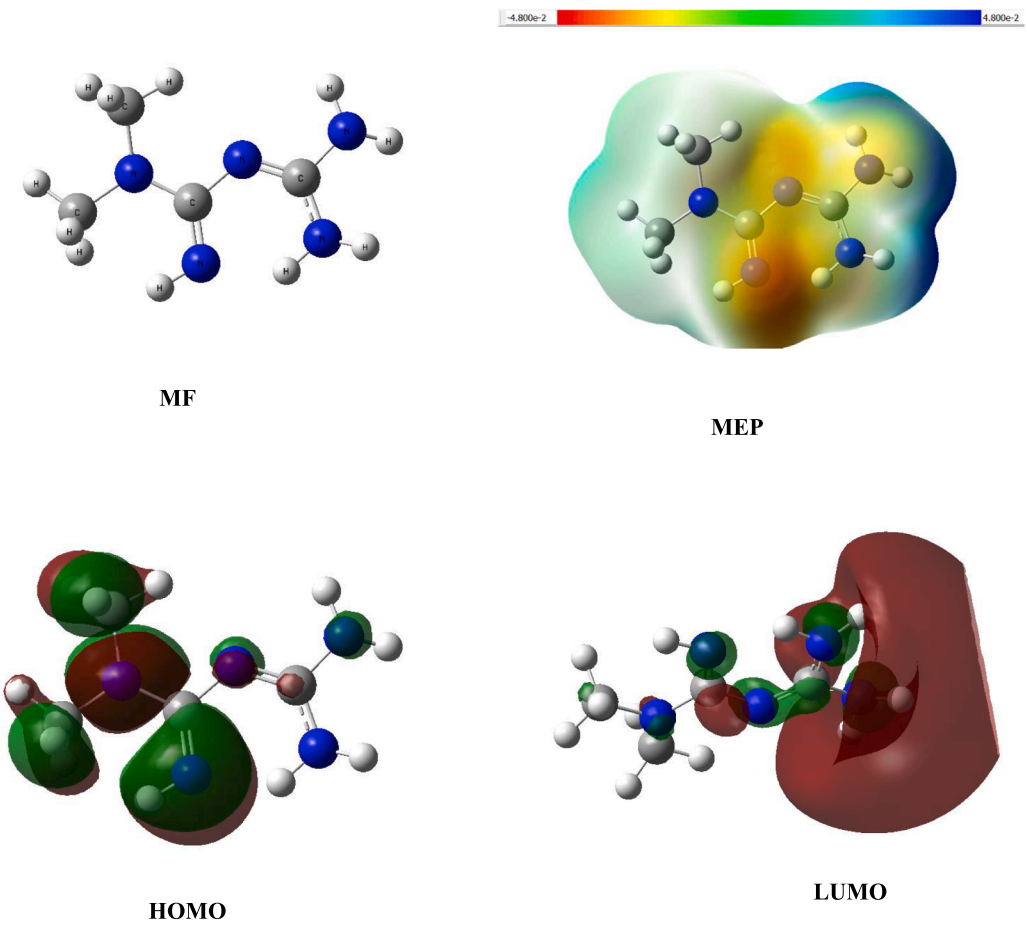

Fig. 1. Optimized structure, MEP plot, and FMO plot (HOMO and LUMO) of the MF molecule (the color scheme for MEP surface is red-electron rich or partially negative charge; blue-electron deficient or partially positive charge; light blue-slightly electron deficient region; yellow-slightly electron rich region, respectively).

addition, BN nanoclusters have excellent adsorption properties, which have been studied experimentally and computationally by numerous researchers [18–21], studying the adsorption of multiple molecules such as CO, HCN, SCN, Phenol and phenol, etc. $B_{12}N_{12}$ has shown its potential as a sensor [18,22–24], $B_{12}N_{12}$ has demonstrated great stability as a collector of noble gases [25], and many studies have been done about the performance of the $B_{12}N_{12}$ cluster in the adsorption of various drugs [26–34].

Many strategies were studied to improve (BN)x properties, doping atoms of group III or transition metals (replace a new atom with one Bohr atom) [35–37], encapsulating various atoms in BN nanocage [38,39].

Influence of alkali metal doping or trapping on NLO (nonlinear optical) and electronic properties of organic $B_{10}H_{14}$basket [40], conjugated aromatic rings [41], $Al_{12}N_{12}$ nanoclusters [42], and $C_{60}Cl_8$ [43] have been reported and shown to be effective in improving their properties. Recently, Shakerzadeh et al. [44] showed that the encapsulation of alkali metals in the group III nitrides could adjust the NLO and electronic features of these nanoclusters. The recent work reported by Huang et al. [45] indicated the computational study of D-Penicillamine adsorption onto BN surface doped with Al and Ga for drug delivery. The designed material showed promising performance for drug delivery applications.

Here we trapped alkali metal atoms (Li, Na, and K) on $B_{12}N_{12}$ clusters and studied the interaction of MF molecule on the surface of nanoclusters, in comparison with pure $B_{12}N_{12}$ within their structural and electronic properties. It has been observed that encapsulation with the group I metals has an influence on the features of these nanoclusters.

2. Computational methods

Full geometry optimization of the MF (metformin) molecule, considerable M@$B_{12}N_{12}$(M = Li, Na, K) nanoclusters and their various state of interactions were performed using B3LYP functional with 6–311++G (d, p) basis set based on density functional theory (DFT) [45–47]. Frequency analysis was performed, and no imaginary frequencies were seen for all states. The restricted approach is applied for geometry optimization and electronic features investigation of pure $B_{12}N_{12}$ and the spin-unrestricted method for encapsulated clusters. Molecular electrostatic potential (MEP), natural bond orbital (NBO) [48,49]and, frontier molecular orbital (FMO) analysis was carried out via the Gaussian09 package [50,51] to investigate the crucial parameters. Basis set superposition error (BSSE) calculations were performed for all states. The density of states (DOS) plots were calculated using the GaussSum program [52]. The GaussView code [53] was used as a visualized program for the optimized structures and charge density distributions [45].

the adsorption energies (E_{ads}) of metformin molecule over the pure $B_{12}N_{12}$ fullerene and encapsulated cages are represented by [45]:

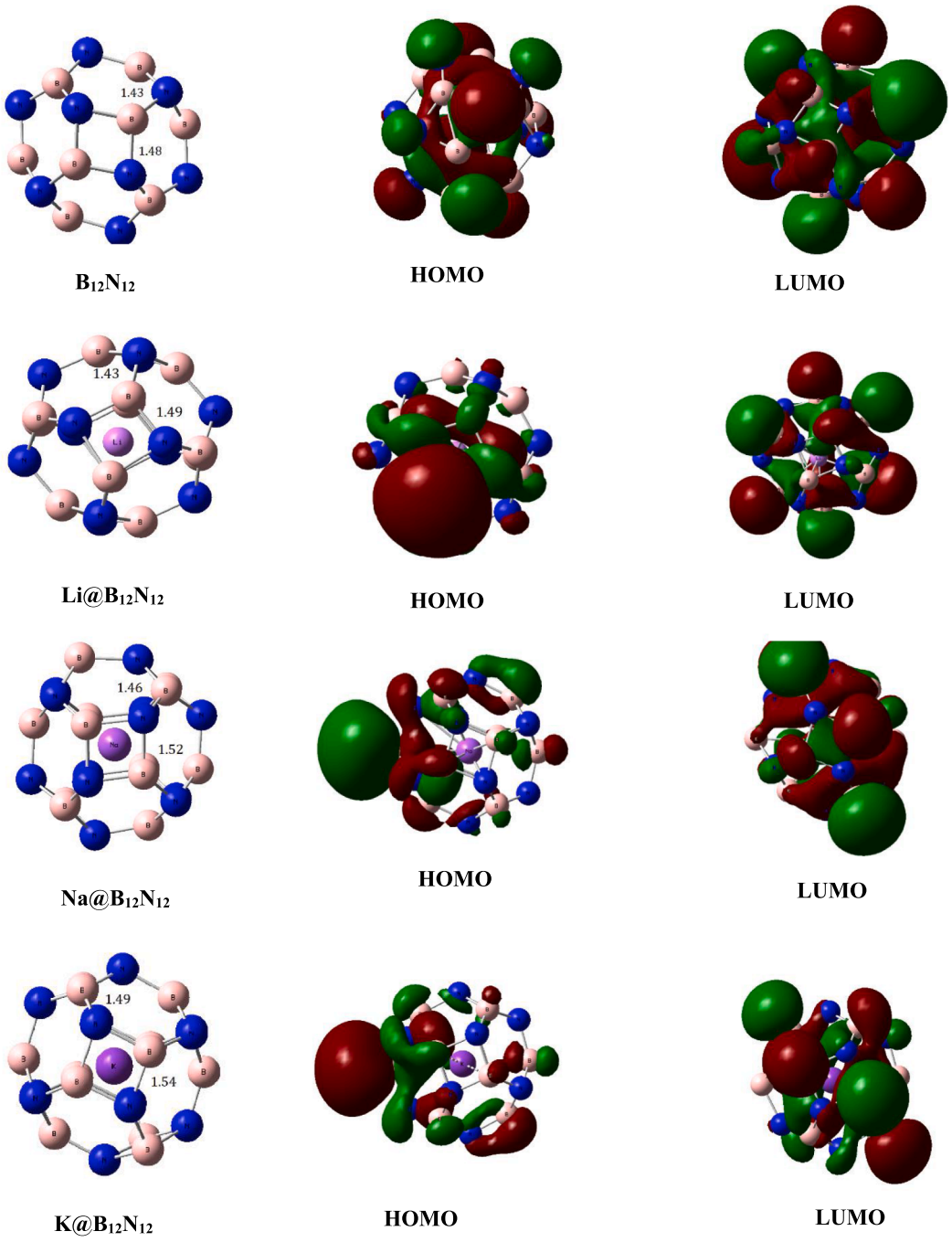

Fig. 2. The optimized geometries of $Li@B_{12}N_{12}$, $Na@B_{12}N_{12}$, $K@B_{12}N_{12}$ and the contour plots of HOMO and LUMO of the considered complexes.

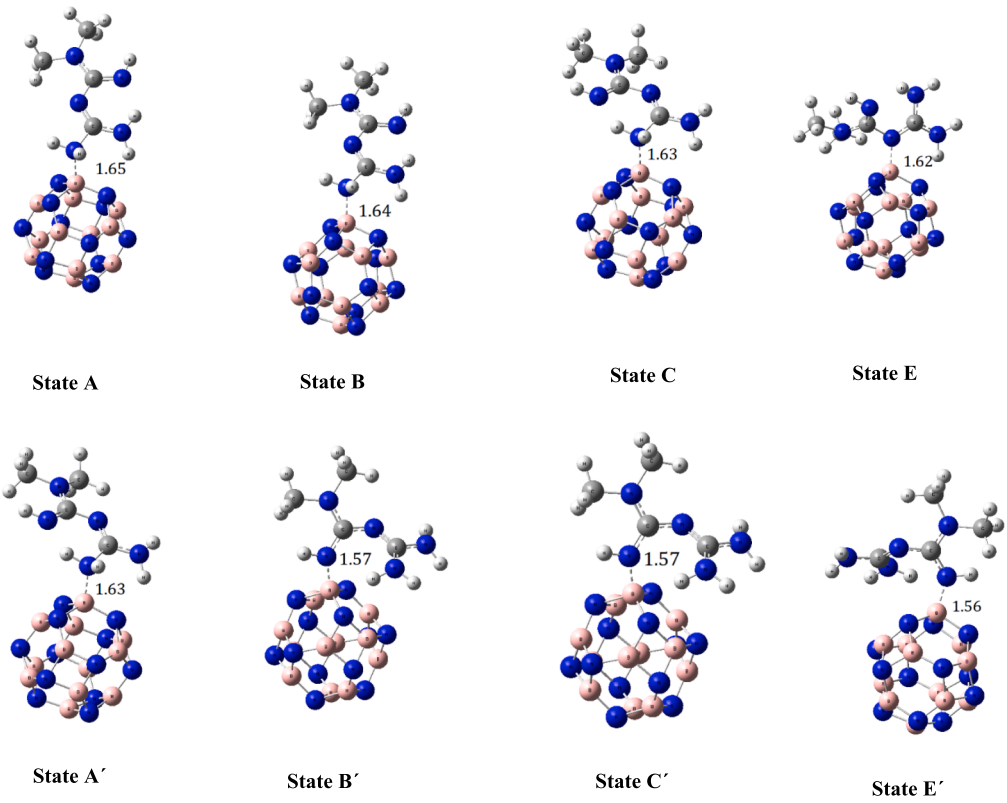

Fig. 3. Optimized geometry of the metformin drug absorption with NH_2(states A-E) and the metformin drug absorption with NH (state A´-E´) groups upon the pure $B_{12}N_{12}$ fullerene.

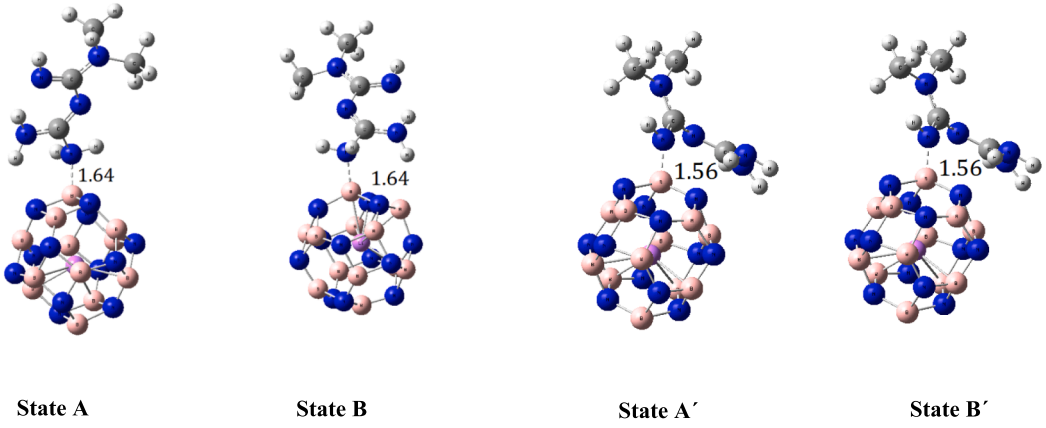

Fig. 4. Optimized geometries of the MF interacting with Li@B12N12 fullerene.

$$E_{ads} = E_{MF/cage} - \left(E_{cage} + E_{MF}\right) + E_{BSSE} \quad (1)$$

where E_{MF} is the total energy of the MF molecule, and E_{cage} is the total energy of pristine and $M@B_{12}N_{12}$ clusters. $E_{MF/cage}$ is the total energy of considrable clusters loaded with the MF drug [45].

The thermodynamic parameters of metformin adsorption over nanocages, the Gibbs free energy (ΔG), enthalpy (ΔH), and entropy (ΔS) magnitude of adsorption per molecule, were also calculated at 298 K and 1 atm using B3LYP /6–311++G (d, p) computational method.

Based on the Koopman theory [54], the physicochemical features of investigated complexes were evaluated by defining the energies of the highest occupied molecular orbital (HOMO) and the lowest unoccupied molecular orbital (LUMO) according to the following equations [45]:

$$\mu = -\frac{I + A}{2} \quad (2)$$

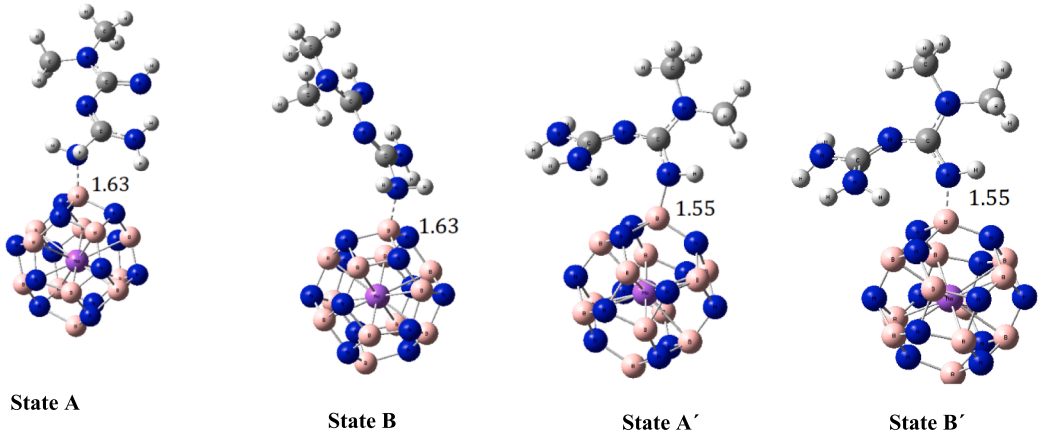

Fig. 5. Optimized geometries of the MF interacting with Na@B12N12 fullerene.

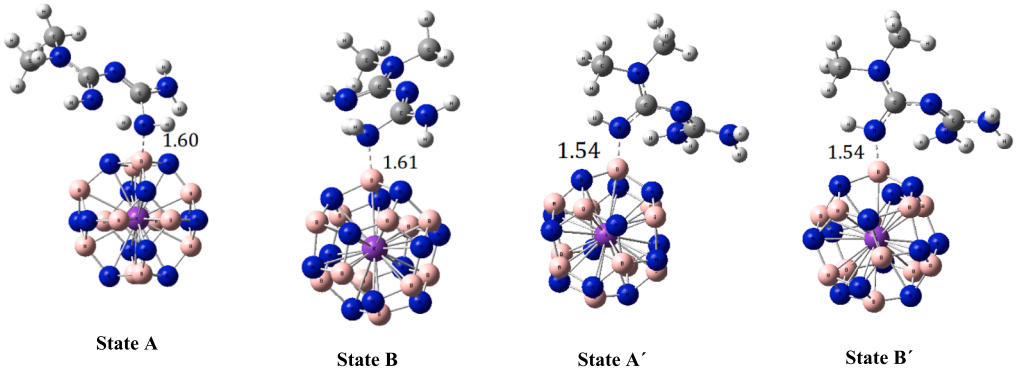

Fig. 6. Optimized geometries of the MF interacting with K@B12N12 fullerene.

Table 1
Calculated adsorption energy (E_{ads}), dipole moment (μ_D), HOMO energy (E_{HOMO}), LUMO energy (E_{LUMO}), energy gap (E_{gap}), and quantum molecular descriptors for MF, $B_{12}N12$, Li@B11N12 and Na@B11N12 and K@B12N12and the most stable state of MF/ M@B11N12.

Property	E_{ads} (eV)	μ_DDeby	E_{HOMO}(eV)	E_{LUMO}(eV)	E_{gap}(eV)	I (eV)	A (eV)	χ(eV)	μ(eV)	η(eV)	S (eV^1)	ω(eV)
MF	–	1.17	−0.25	−0.01	0.21	0.25	0.01	0.11	−0.11	0.10	4.78	0.06
$B_{12}N_{12}$	–	0.00	−0.29	−0.04	0.25	0.29	0.04	0.17	−0.17	0.12	4.06	0.16
State C	−0.93	7.39	−0.24	−0.05	0.19	0.24	0.05	0.14	−0.14	0.09	5.26	0.11
State E	−1.03	9.74	−0.25	−0.04	0.21	0.25	0.04	0.14	−0.14	0.10	4.76	0.10
State C´	−2.08	10.22	−0.24	−0.04	0.20	0.24	0.04	0.14	−0.14	0.10	5.00	0.10
State E´	−2.14	19.38	−0.25	−0.04	0.21	0.25	0.04	0.14	−0.14	0.10	4.95	0.10
Li@$B_{11}N_{12}$	–	2.89	−0.16	−0.06	0.10	0.16	0.06	0.11	−0.11	0.05	10.52	0.12
State A	−1.61	11.04	−0.13	−0.05	0.08	0.13	0.05	0.09	−0.09	0.04	12.50	0.10
State B	−1.71	6.04	−0.15	−0.05	0.10	0.15	0.05	0.10	−0.10	0.05	10.00	0.10
State A´	−2.23	14.44	−0.12	−0.05	0.07	0.12	0.05	0.08	−0.08	0.04	14.28	0.09
State B´	−2.24	6.04	−0.15	−0.05	0.10	0.15	0.05	0.10	−0.10	0.05	10.00	0.10
Na@$B_{11}N$	–	3.47	−0.15	−0.07	0.08	0.15	0.07	0.11	−0.11	0.04	12.35	0.14
State A	−1.68	11.72	−0.13	−0.06	0.07	0.13	0.06	0.09	−0.09	0.03	14.28	0.13
State B	−1.69	11.60	−0.13	−0.06	0.07	0.13	0.06	0.09	−0.09	0.03	14.28	0.13
State A´	−2.30	15.21	−0.11	−0.05	0.06	0.11	0.05	0.08	−0.08	0.03	16.66	0.10
State B´	−2.30	15.20	−0.11	−0.05	0.06	0.11	0.05	0.08	−0.08	0.03	16.67	0.11
K@$B_{11}N_{12}$	–	3.30	−0.15	−0.08	0.07	0.15	0.08	0.12	−0.12	0.04	13.12	0.17
State A	−1.83	7.21	−0.12	−0.05	0.07	0.12	0.05	0.08	−0.08	0.03	14.28	0.10
State B	−1.80	9.66	−0.12	−0.06	0.06	0.12	0.06	0.09	−0.09	0.03	16.66	0.13
State A´	−2.38	9.78	−0.11	−0.05	0.06	0.11	0.05	0.08	−0.08	0.03	16.66	0.10
State B´	−2.38	9.78	−0.12	−0.05	0.07	0.16	0.05	0.08	−0.08	0.03	14.71	0.10

Table 2
Calculated enthalpy change (ΔH_{ads}), Gibbs free energy change (ΔG_{ads}), entropy change (ΔS_{ads}) at 298 K and 1 atm, minimum vibrational frequencies (ν_{min}) and maximum vibrational frequencies (ν_{max}).

Property	$\Delta G(eV)$	$\Delta H(eV)$	$\Delta S(eV/K)$	$\nu_{min} cm^{-1}$	$\nu_{max} cm^{-1}$
MF	–	–	–	61.76	3677.63
$B_{12}N_{12}$	–	–	–	324.36	1441.61
State C	−0.16	−0.09	−0.0002	19.34	3553.67
State E	−0.17	−0.19	0.0007	22.54	3676.13
State C′	−0.21	−0.23	0.0006	7.28	3699.1
State E′	−0.21	−0.23	0.0006	19.38	3707.83
$Li@B_{11}N_{12}$	–	–	–	306.37	1431.49
State A	−0.30	−0.86	0.0018	19.14	3564.27
State B	−0.40	−0.96	0.0018	16.62	3562.86
State A′	−0.96	−1.47	0.0017	11.58	3693.27
State B′	−0.98	−1.48	0.0017	16.62	3562.86
$Na@B_{11}N$	–	–	–	352.65	1396.77
State A	−0.37	−0.93	0.0018	19.23	3564
State B	−0.38	−0.93	0.0018	18.36	3563.75
State A′	−1.02	−1.55	0.0017	19.24	3699.77
State B′	−1.02	−1.55	0.0017	19.39	3699.93
$K@B_{11}N_{12}$	–	–	–	396.57	1314.5
State A	−0.55	−1.11	0.0018	15.47	3646.73
State B	0.54	−1.08	0.0018	17.30	3653.07
State A′	−1.11	−1.63	0.0017	17.38	3694.09
State B′	−1.11	−1.63	0.0017	17.37	3694.12

$$\mu = -x \tag{3}$$

$$\eta = \frac{1}{2}(I - A) \tag{4}$$

$$S = \frac{1}{2\eta} \tag{5}$$

$$\omega = \frac{\mu^2}{2\eta} \tag{6}$$

where I ($-E_{HOMO}$) and A ($-E_{LUMO}$) are the ionization potential and the electron affinity of the system respectively. μ is chemical potential, x the electronegativity, η the global hardness, S the global softness and based on Parr et al [55] definition, ω is electrophilicity [45].

3. Result and discussion

Fig. 1 presents MEP and FMO plots of the optimized metformin molecule. Based on MEP calculation, rich or partially negative charge (red and yellow regions) is observed around nitrogen atoms and partially positive charge (blue and light blue regions) is seen around carbon atoms. Hence the metformin illustrates two nucleophilic sites for interaction with cluster, NH_2 and NH.

Herein, alkali metal atoms were trapped in the $B_{12}N_{12}$ and new clusters are examined using the DFT method. In this regard, the metal atom of group I is placed in the center of the cage structure. The diameters of the structures are plotted, and the metal atom is at the intersection of the diameters. Full geometry optimization has been carried out at B3LYP/6–311++G (d, p) computational level [44]. The optimized structures of pure $B_{12}N_{12}$ and encapsulated nanoclusters ($M@B_{12}N_{12}$, M = Li, Na, K) are presented in Fig. 2. From this figure, it can be seen that alkali atoms are located almost at the center of the structures after optimization. It can be noticed that each nanocluster contains hexagonal and tetragonal rings, and two types of B-N bonds are distinguished. The common bond among hexagonal rings (hh) and the bond that joint one tetragonal and hexagonal (hs) ring together. hh B-N bond lengths are 1.43, 1.43, 1.46 and 1.49 Å, and the comparable hs bonds lengths are 1.48, 1.49, 1.52 and 1.54 Å for $B_{12}N_{12}$, $Li@B_{12}N_{12}$, $Na@B_{12}N_{12}$ and $K@B_{12}N_{12}$ nanoclusters respectively, with a sp^2 orbital hybridization. Our calculations agree with the results of reported theoretical data. The hs bond length value is more than the corresponding hh bond because the involvement of the p orbital in hs bonds is larger than hh bonds[44]. In all investigated cages atomic sites are equivalent. First, we examined four states for the interactions of the MF molecule over the surface of the pure cluster $B_{12}N_{12}$. Next, metformin molecule nears various sites of the cluster, comprising the B or N atom, the bridging site of the hh or hs bond, and over the center of different rings, via NH or NH_2. Four states for drug adsorption via the NH_2 group upon $B_{12}N_{12}$ (A-E) and four states via the NH group (A′-E′) were optimized, obtained configurations are depicted in Fig. 3. After optimization two stable and recognizable complexes are acquired for each nucleophilic site. Optimum configurations of drug interaction with encapsulation clusters, $Li@B_{12}N_{12}$, $Na@B_{12}N_{12}$, and $K@B_{12}N_{12}$ are presented in Figs. 4, 5, and 6, respectively. The best interaction distances are also determined. Based on the above results, the interaction of MF molecules on the surface of encapsulated clusters was performed and adsorption energies (E_{ads}) were obtained using Eq. (1) for each state (Table1). The negative binding energies show that the interaction of drug molecule with complexes have exothermic nature. The most negative adsorption energies belong to the interaction of the NH nucleophile site, which forms a strong covalently binding to the Bohr atom of $B_{12}N_{12}$, $Li@B_{12}N_{12}$, $Na@B_{12}N_{12}$, and $K@B_{12}N_{12}$ nanoclusters with the value of −2.14, −2.22, −2.30 and, −2.38 eV respectively [45].

NBO analysis indicates that strong interactions are existed between metformin and cluster, due to the rich electron sites of the drug (NH and NH_2 group) and the empty 2p valence shell of the Bohr atom, so, a large charge transfer occurs between the drug and the considered cluster, from MF to cage. Hence, MF is defined as an electron donor, and the cluster is defined as an acceptor. It is noticed that due to the trapping of

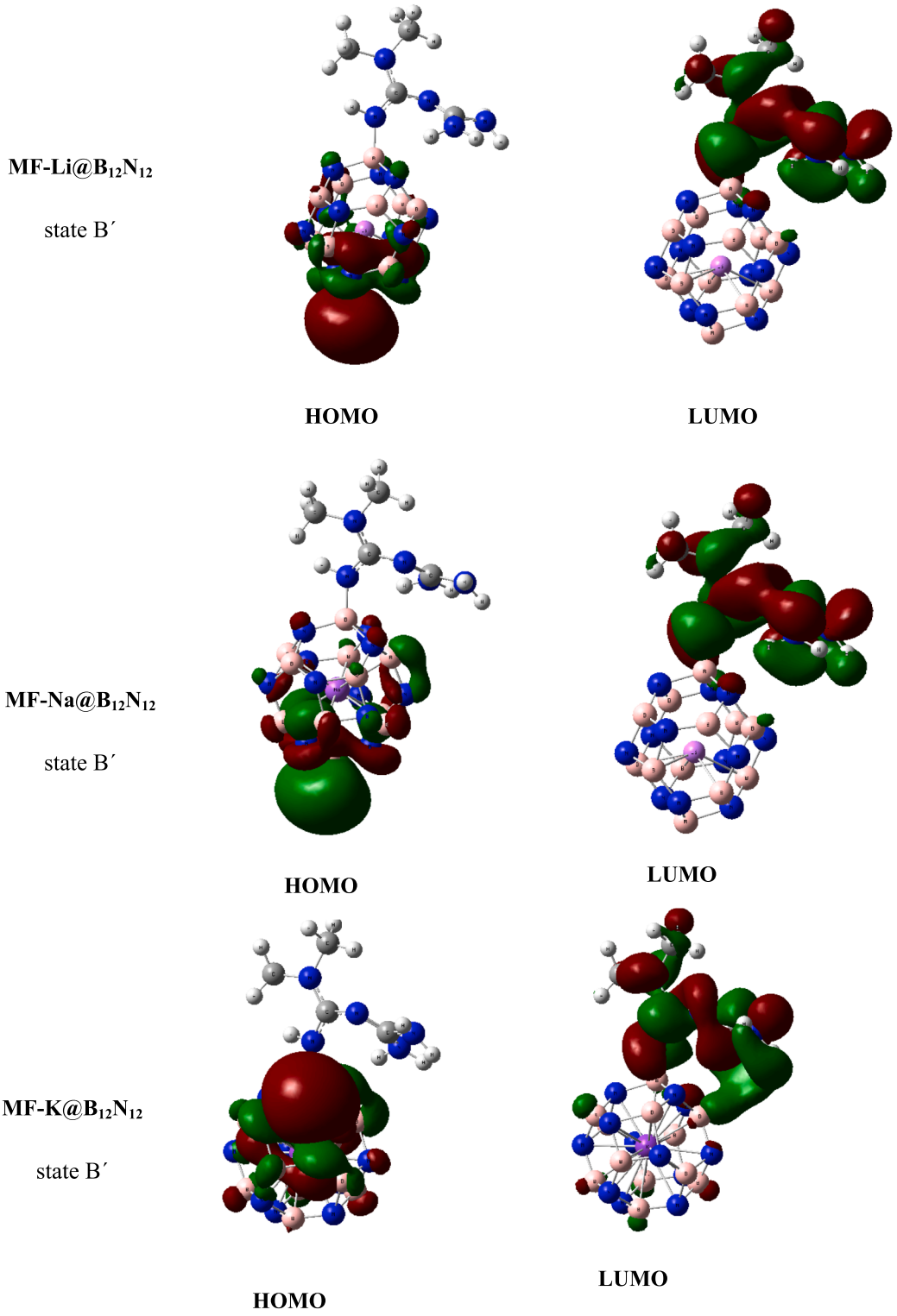

Fig. 7. The typically contour plots of HOMO and LUMO of the best structures of the MF interacting with the $Li@B_{12}N_{12}$, $Na@B_{12}N_{12}$, $K@B_{12}N_{12}$ systems.

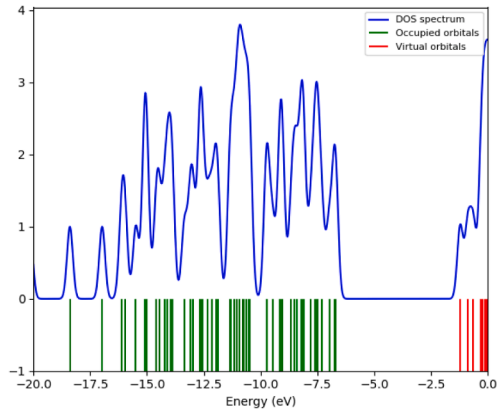

$B_{12}N_{12}$

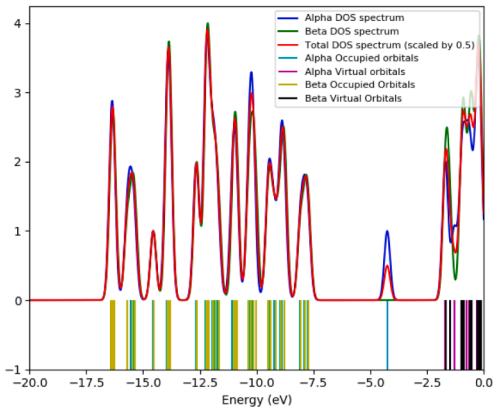

$Li@B_{12}N_{12}$

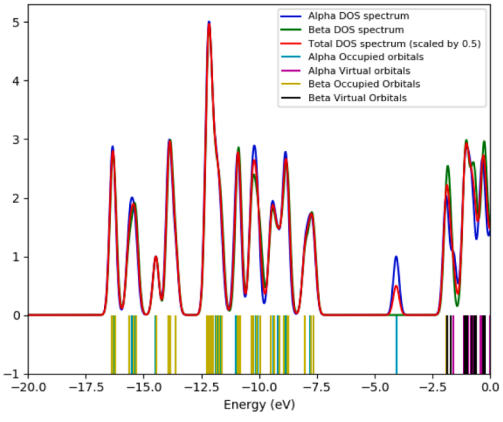

$Na@B_{12}N_{12}$

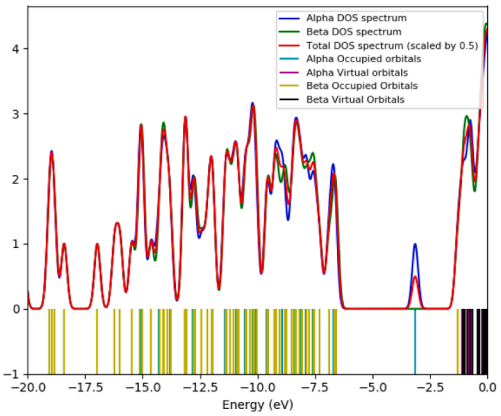

$K@B_{12}N_{12}$

Fig. 8. DOS plots of pure $B_{12}N_{12}$, $Li@B_{12}N_{12}$, $Na@B_{12}N_{12}$, $K@B_{12}N_{12}$ nanoclusters.

alkali metal atoms within the $B_{12}N_{12}$ nanocages, the adsorption energies for $Li@B_{12}N_{12}$, $Na@B_{12}N_{12}$, and $K@B_{12}N_{12}$ increase, respectively. According to charge computations, transferring the diffuse excess electrons to the BN fullerene from the metal atom, change the electronic attributes of the deemed clusters and consequently, the adsorption energies of complexes. The $K@B_{12}N_{12}$ configuration shows impressively the largest E_{ads} among the considered configurations. Based on the obtained dipole moments (Table 1), the polarization of doped clusters increases after drug adsorption. Adsorption functionals via the NH nucleophile site have higher dipole moments than the NH_2 group in all encapsulated clusters, confirming their more excellent stability.

Next, thermodynamic parameters (ΔH_{ads}, ΔG_{ads}, and ΔS_{ads}) were obtained at 298 K, and values are given in Table 2. Negative magnitudes show that drug molecule adsorption is an exothermic reaction. As we can see, thermodynamic energies became more hostile with the trapping of alkali metals in pristine $B_{12}N_{12}$, and an increasing trend is observed by the atomic number enhancement of alkali metals. Fig. 7 shows the HOMO (highest occupied molecular orbital) and LUMO (lowest unoccupied molecular orbital) molecular orbitals of adsorbed metformin (in the different states) over pristine and encapsulated fullerenes. The green color orbitals imply positive regions, and the red colors imply negative regions. In all states, the HOMO orbitals are located on the Nitrogen and Bohr atoms of clusters, and the LUMO orbitals are localized on metformin and B atoms of cages. The corresponding HOMO and LUMO energies and HOMO–LUMO gap ($E_{gap} = E_{LUMO}–E_{HOMO}$) of the optimized structures are summarized in Table 1. The fullerene has an energy band gap (E_{gap}) of 6.48 eV, which is similar to data from other reports [37]. Encapsulation reduces the energy gaps of obtained clusters more than pristine $B_{12}N_{12}$. Systems with smaller energy gaps tend to be more reactive and less stable from the kinetic point of view [45]. Therefore, the incorporation of the Li, Na, and K atoms into the $B_{12}N_{12}$ structure enhances the adsorption energies of functionalized systems, confirming the decline in HOMO–LUMO gaps.

Next, based on HOMO and LUMO energies, quantum molecular descriptors (Eqs. (2)–(6)) were obtained for MF adsorption on considerable nanoclusters that are reported in Table 1. It is observed.

that by encapsulating the alkali metal atoms in the $B_{12}N_{12}$ cage, a reduction trend is observed with the increase in atomic radius or atomic

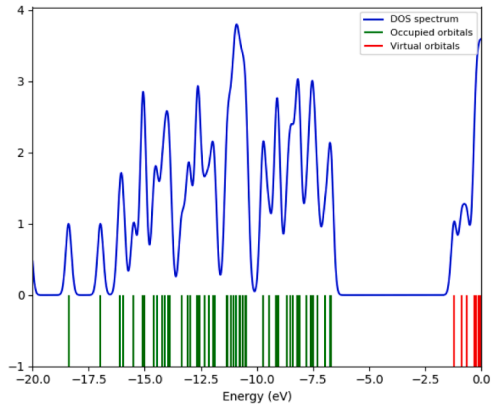

MF -$B_{12}N_{12}$

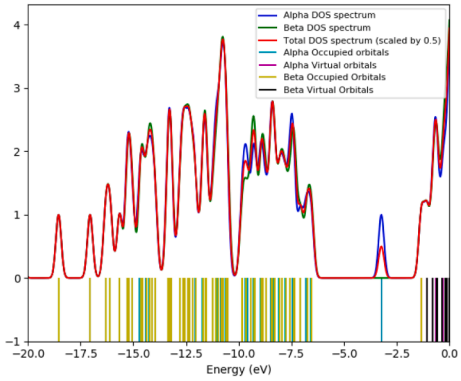

MF-Li@$B_{12}N_{12}$

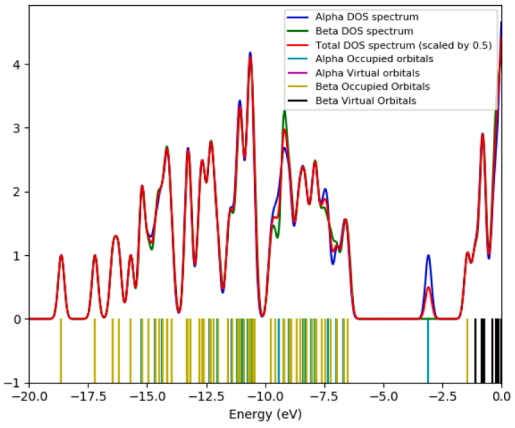

MF-Na@$B_{12}N_{12}$

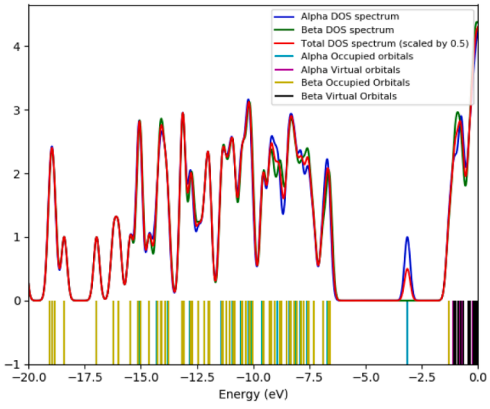

MF-K@$B_{12}N_{12}$

Fig. 9. DOS plots of the best structures of the MF interacting with the pure $B_{12}N_{12}$, Li@$B_{12}N_{12}$, Na@$B_{12}N_{12}$, K@$B_{12}N_{12}$ systems.

number, so the global hardness also shows the reduction trend, confirming the increase in adsorption energies.

For further investigation, the density of states (DOS) was examined for all functionals. The DOS spectrums presented in Figs. 8 and 9, illustrate that $B_{12}N_{12}$ and Li@$B_{12}N_{12}$, Na@$B_{12}N_{12}$, and K@$B_{12}N_{12}$ have semiconducting features, and also show the decrease of E_{gap} upon the adsorption process in continuation of previous results in this work.

To better understand the nature of adsorption of MF molecules on the pure $B_{12}N_{12}$ and M@$B_{12}N_{12}$(M = Li, Na, K) fullerenes, the topology variance in the electron localization function (ELF) of the best state of each encapsulation cluster was analyzed. A good electron space delocalization between the drug and the considered clusters is observed. The ELF of the jellium-like homogeneous electron gas has an order of magnitude $0 \leq ELF \leq 1$. ELF = 1.0 is related to covalent bonds and lone pair electrons (red areas), ELF = 0.50 corresponds to free electrons gas behavior (green areas), and 0.0 shows no localization [56]. ELF contour plots of the MF molecule adsorption on the $B_{12}N_{12}$, Li@$B_{12}N_{12}$, Na@$B_{12}N_{12}$, and K@$B_{12}N_{12}$ fullerenes are displayed in Fig. 10. Significant localization is observed among the N element of the drug and the Bohr element of the encapsulated nanoclusters (red areas), resulting in strong covalent binding in the respective states. The electrons are fully localized among the nitrogen atom of the MF molecule and the surface of the nanoclusters, where they share some electrons. As displayed in Fig. 6 the larger ELF value (Z≈ 1.0) located on the B-N bonds, exhibits a chemical covalent bond that can be formed through the MF molecule adsorption on the pure and encapsulated fullerenes [57].

4. Conclusion

A comprehensive DFT study at the B3LYP/6–311++G (d, p) level indicates, trapping Li, Na, and K metals on the $B_{12}N_{12}$ structure can significantly intensify the adsorption ability of the metformin drug compared to the pure $B_{12}N_{12}$ cage. Through NBO results two nucleophilic sites, NH and NH_2 groups, of the MF drug as doner of electrons interact to empty Bohr atomic orbitals of clusters as acceptors. The analysis illustrates that interactions of the NH group formed the most stable configurations compared to the NH2. HOMO-LUMO energy gaps and DOS plots introduce considered complexes as semiconductors,

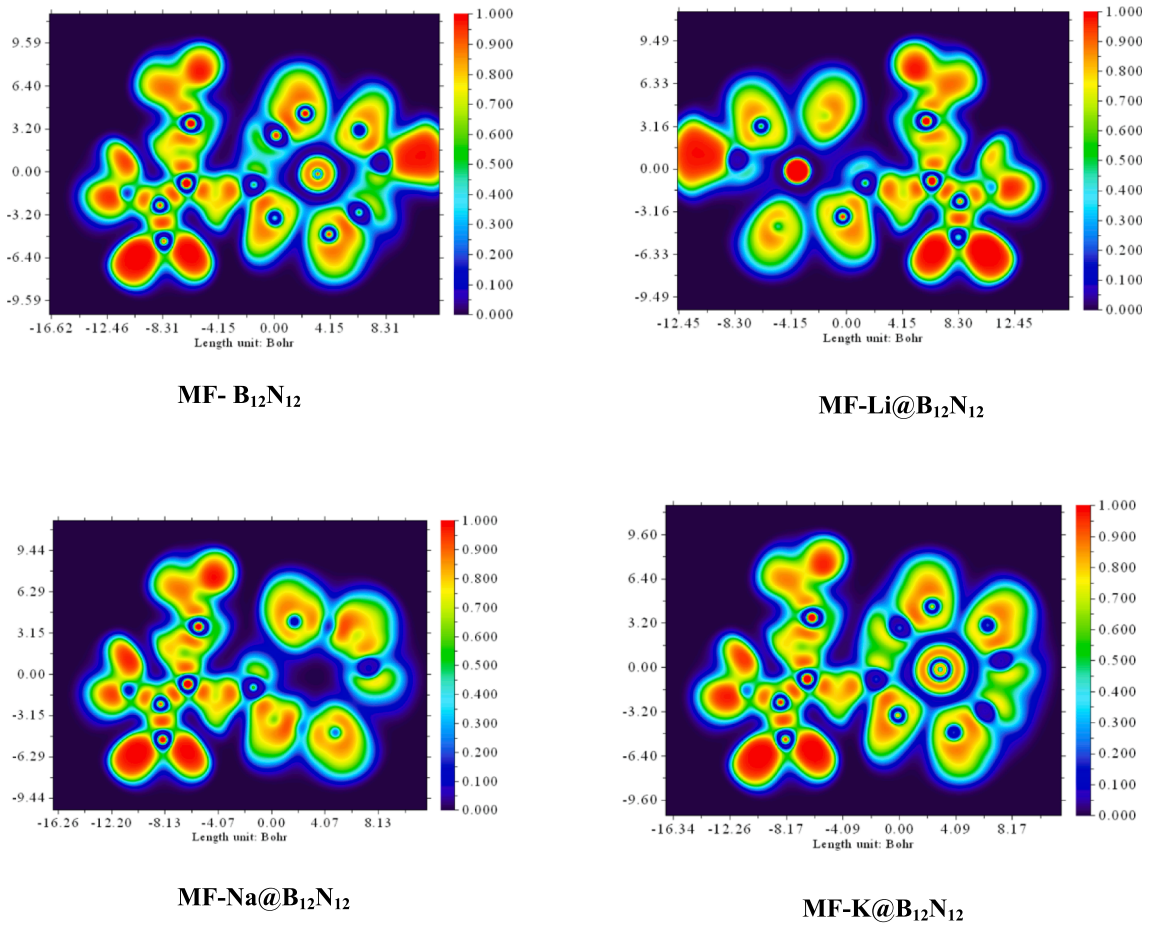

Fig. 10. Electron Localization Function the best structures of the MF interacting with the Li@$B_{12}N_{12}$, Na@$B_{12}N_{12}$, K@$B_{12}N_{12}$ systems.

whose gap energies decrease with encapsulation of Li, Na, and K. Thermodynamic parameters calculation shows an exothermic reaction via MF adsorption. Obtained adsorption energies and thermochemistry parameters exhibit a strong interaction and exothermic reaction between drug and clusters. The quantum molecular descriptors are calculated, and a reduction trend in the global hardness besides an increase of adsorption energies is observed by increasing in atomic radius of trapped metals, in addition, the encapsulated clusters have higher reactivity than pure $B_{12}N_{12}$.

CRediT authorship contribution statement

Ying Lai: Writing – original draft, Validation, Resources, Conceptualization. **Tariq J. Al-Musawi:** Conceptualization, Formal analysis, Methodology. **Uday Abdul-Reda Hussein:** Writing – original draft, Software, Resources. **Ibrahem Waleed:** Conceptualization, Writing – original draft, Formal analysis. **Hanan Hassan Ahmed:** Writing – review & editing, Validation, Investigation. **Anwar Qasim Khallawi:** Formal analysis, Writing – review & editing, Methodology. **Khulood Majid Alsaraf:** Writing – review & editing, Validation, Investigation. **Mohammed Asiri:** Formal analysis, Methodology, Resources, Writing – review & editing. **Munther Abosaooda:** Conceptualization, Writing – review & editing, Investigation. **Hashem O. Alsaab:** Funding acquisition, Writing – original draft, Formal analysis, Writing – review & editing.

Declaration of Competing Interest

The authors declare that they have no known competing financial interests or personal relationships that could have appeared to influence the work reported in this paper.

Data availability

No data was used for the research described in the article.

Acknowledgments

Hashem O. Alsaab would like to acknowledge Taif University Researchers Supporting Project number (TURSP-2020/67), Taif University, Taif, Saudi Arabia.

References

[1] A.J. Scheen, Clinical pharmacokinetics of metformin, Clin. Pharmacokinet. 30 (1996) 359–371.
[2] K. Mahmood, M. Naeem, N.A. Rahimnajjad, Metformin: the hidden chronicles of a magic drug, Eur. J. Intern. Med. 24 (1) (2013) 20–26.
[3] C.V. Rizos, M.S. Elisaf, Metformin and cancer, Eur. J. Pharmacol. 705 (1–3) (2013) 96–108.
[4] R. Dowling, et al., Metformin in cancer: translational challenges, J. Mol. Endocrinol. 48 (3) (2012) R31–R43.
[5] J.L. Wright, J.L. Stanford, Metformin use and prostate cancer in Caucasian men: results from a population-based case–control study, Cancer Causes Control 20 (2009) 1617–1622.
[6] Z. Liu, et al., In vivo biodistribution and highly efficient tumour targeting of carbon nanotubes in mice, Nat. Nanotechnol. 2 (1) (2007) 47–52.
[7] Z. Liu, et al., In vivo Biodistribution and Highly Efficient Tumour Targeting of Carbon Nanotubes in Mice, in: Nano-Enabled Medical Applications, Jenny Stanford Publishing, 2020, pp. 403–429.
[8] Z. Liu, et al., Carbon nanotubes in biology and medicine: in vitro and in vivo detection, imaging and drug delivery, Nano Res. 2 (2009) 85–120.
[9] D.A. Heller, et al., Single-walled carbon nanotube spectroscopy in live cells: towards long-term labels and optical sensors, Adv. Mater. 17 (23) (2005) 2793–2799.

[10] X. Sun, et al., Nano-graphene oxide for cellular imaging and drug delivery, Nano Res. 1 (2008) 203–212.
[11] J. Shi, et al., PEI-derivatized fullerene drug delivery using folate as a homing device targeting to tumor, Biomaterials 34 (1) (2013) 251–261.
[12] A. Merlo, et al., Boron nitride nanomaterials: biocompatibility and bio-applications, Biomater. Sci. 6 (9) (2018) 2298–2311.
[13] X. Chen, et al., Boron nitride nanotubes are noncytotoxic and can be functionalized for interaction with proteins and cells, J. Am. Chem. Soc. 131 (3) (2009) 890–891.
[14] S.-H. Xu, et al., Stability and property of planar (BN) x clusters, Chem. Phys. Lett. 423 (1–3) (2006) 212–214.
[15] G. Seifert, et al., Boron-nitrogen analogues of the fullerenes: electronic and structural properties, Chem. Phys. Lett. 268 (5–6) (1997) 352–358.
[16] D.L. Strout, Structure and stability of boron nitrides: isomers of B12N12, Chem. A Eur. J. 104 (15) (2000) 3364–3366.
[17] D.L. Strout, Structure and stability of boron nitrides: the crossover between rings and cages, Chem. A Eur. J. 105 (1) (2001) 261–263.
[18] F. Zhao, et al., C-doped boron nitride fullerene as a novel catalyst for acetylene hydrochlorination: a DFT study, RSC Adv. 5 (69) (2015) 56348–56355.
[19] J. Beheshtian, et al., Toxic CO detection by B12N12 nanocluster, Microelectron. J. 42 (12) (2011) 1400–1403.
[20] J. Beheshtian, et al., B12N12 nano-cage as potential sensor for NO2 detection, Chin. J. Chem. Phys. 25 (1) (2012) 60.
[21] M.R.S.A. Janjua, Theoretical framework for encapsulation of inorganic B12N12 nanoclusters with alkaline earth metals for efficient hydrogen adsorption: a step forward toward hydrogen storage materials, Inorg. Chem. 60 (4) (2021) 2816–2828.
[22] M.D. Esrafili, P. Nematollahi, R. Nurazar, A comparative study of the CO oxidation reaction over pristine and C-doped boron nitride fullerene, RSC Adv. 6 (21) (2016) 17172–17178.
[23] A. Soltani, et al., Adsorption of cyanogen chloride over Al-and Ga-doped BN nanotubes, Superlattice. Microst. 75 (2014) 564–575.
[24] A. Soltani, et al., Ab initio investigation of Al-and Ga-doped single-walled boron nitride nanotubes as ammonia sensor, Appl. Surf. Sci. 263 (2012) 619–625.
[25] M.S. Hoseininezhad-Namin, et al., Ab initio study of TEPA adsorption on pristine, Al and Si doped carbon and boron nitride nanotubes, J. Inorg. Organomet. Polym Mater. 30 (2020) 4297–4310.
[26] M.T. Baei, et al., A computational study of adenine, uracil, and cytosine adsorption upon AlN and BN nano-cages, Phys. B Condens. Matter 444 (2014) 6–13.
[27] M.D. Esrafili, R. Nurazar, Methylamine adsorption and decomposition on B12N12 nanocage: A density functional theory study, Surf. Sci. 626 (2014) 44–48.
[28] A. Bahrami, et al., A first-principles study on the adsorption behavior of amphetamine on pristine, P-and Al-doped B12N12 nano-cages, Superlattice. Microst. 64 (2013) 265–273.
[29] M.B. Javan, et al., A DFT study on the interaction between 5-fluorouracil and B 12 N 12 nanocluster, RSC Adv. 6 (106) (2016) 104513–104521.
[30] A. Soltani, et al., Electronic and optical properties of 5-AVA-functionalized BN nanoclusters: a DFT study, New J. Chem. 40 (8) (2016) 7018–7026.
[31] Y. Cao, et al., Penicillamine functionalized B12N12 and B12CaN12 nanocages act as potential inhibitors of proinflammatory cytokines: A combined DFT analysis, ADMET and molecular docking study, Arab. J. Chem. 14 (7) (2021), 103200.
[32] E. Shakerzadeh, A DFT study on the formaldehyde (H2CO and (H2CO) 2) monitoring using pristine B12N12 nanocluster, Physica E 78 (2016) 1–9.
[33] A.R. Soltani, M.T. Baei, A DFT study on structure and electronic properties of BN nanostructures adsorbed with dopamine, Computation 7 (4) (2019) 61.
[34] S. Kaviani, S. Shahab, M. Sheikhi, Adsorption of alprazolam drug on the B12N12 and Al12N12 nano-cages for biological applications: A DFT study, Physica E 126 (2021), 114473.
[35] S. Larki, et al., The Al, Ga and Sc dopants effect on the adsorption performance of B12N12 nanocluster toward pnictogen hydrides, Chem. Phys. 526 (2019), 110424.
[36] S. Kaviani, et al., A DFT study of Se-decorated B12N12 nanocluster as a possible drug delivery system for ciclopirox, Comput. Theor. Chem. 1201 (2021), 113246.
[37] E. Shakerzadeh, N. Barazesh, S.Z. Talebi, A comparative theoretical study on the structural, electronic and nonlinear optical features of B12N12 and Al12N12 nanoclusters with the groups III, IV and V dopants, Superlattice. Microst. 76 (2014) 264–276.
[38] N. Abdolahi, et al., Gold decorated B12N12 nanocluster as an effective sulfasalazine drug carrier: A theoretical investigation, Physica E 124 (2020), 114296.
[39] M.R.S.A. Janjua, Prediction and understanding: Quantum chemical framework of transition metals enclosed in a B12N12 inorganic nanocluster for adsorption and removal of DDT from the environment, Inorg. Chem. 60 (14) (2021) 10837–10847.
[40] S. Muhammad, et al., Quantum mechanical design and structure of the Li@ B10H14 basket with a remarkably enhanced electro-optical response, J. Am. Chem. Soc. 131 (33) (2009) 11833–11840.
[41] G. Yu, et al., Alkali metal atom-aromatic ring: A novel interaction mode realizes large first hyperpolarizabilities of M@ AR (M= Li, Na, and K, AR= pyrrole, indole, thiophene, and benzene), J. Comput. Chem. 32 (9) (2011) 2005–2011.
[42] M. Niu, et al., Doping the alkali atom: an effective strategy to improve the electronic and nonlinear optical properties of the inorganic Al12N12 nanocage, Inorg. Chem. 53 (1) (2014) 349–358.
[43] L.-J. Wang, et al., The encapsulated lithium effect of Li@ C 60 Cl 8 remarkably enhances the static first hyperpolarizability, RSC Adv. 3 (32) (2013) 13348–13352.
[44] E. Tahmasebi, E. Shakerzadeh, Z. Biglari, Theoretical assessment of the electro-optical features of the group III nitrides (B12N12, Al12N12 and Ga12N12) and group IV carbides (C24, Si12C12 and Ge12C12) nanoclusters encapsulated with alkali metals (Li, Na and K), Appl. Surf. Sci. 363 (2016) 197–208.
[45] J. Huang, et al., DFT study of D-Penicillamine adsorption on Al and Ga doped boron nitride (Al-B11N12 and Ga-B11N12) nanoclusters as drug delivery agents, J. Mol. Liq. 383 (2023), 122056.
[46] A.D. Beeke, Density-functional thermochemistry. III. The role of exact exchange, J. Chem. Phys 98 (7) (1993) 5648–15646.
[47] C. Lee, W. Yang, R.G. Parr, Development of the Colle-Salvetti correlation-energy formula into a functional of the electron density, Phys. Rev. B 37 (2) (1988) 785.
[48] J.E. Carpenter, Extension of Lewis structure concepts to open-shell and excited-state molecular species, University of Wisconsin-Madison, 1987.
[49] F. Weinhold, and J.I. Carpenter, The structure of small molecules and ions, 1988, Plenum New York.
[50] M. Frisch, and F. Clemente, Gaussian 09, revision a. 01, mj frisch, gw trucks, hb schlegel, ge scuseria, ma robb, jr cheeseman, g. Scalmani, V. Barone, B. Mennucci, GA Petersson, H. Nakatsuji, M. Caricato, X. Li, HP Hratchian, AF Izmaylov, J. Bloino, G. Zhe, 2009, p. 20-44.
[51] M. Frisch, et al., 09, Revision D. 01, Gaussian. Inc., Wallingford, CT, 2009.
[52] N.M. O'boyle, A.L. Tenderholt, K.M. Langner, Cclib: a library for package-independent computational chemistry algorithms, J. Comput. Chem. 29 (5) (2008) 839–845.
[53] M. Frisch, et al., Gaussian 16 Rev. B. 01 Release Notes. 2016, Wallingford, CT.
[54] T. Koopmans, Über die Zuordnung von Wellenfunktionen und Eigenwerten zu den einzelnen Elektronen eines Atoms, Physica 1 (1–6) (1934) 104–113.
[55] R.G. Parr, L.v. Szentpály, S. Liu, Electrophilicity index, J. Am. Chem. Soc. 121 (9) (1999) 1922–1924.
[56] A.D. Becke, K.E. Edgecombe, A simple measure of electron localization in atomic and molecular systems, J. Chem. Phys. 92 (9) (1990) 5397–5403.
[57] A. Soltani, et al., Theoretical studies of hydrazine detection by pure and Al defected MgO nanotubes, Physica E 97 (2018) 239–249.